



CHALMERS
UNIVERSITY OF TECHNOLOGY

Observation of high-energy neutrinos from the Galactic plane

Downloaded from: <https://research.chalmers.se>, 2025-06-01 07:58 UTC

Citation for the original published paper (version of record):

Abbasi, R., Ackermann, M., Adams, J. et al (2024). Observation of high-energy neutrinos from the Galactic plane. *Proceedings of Science*, 444

N.B. When citing this work, cite the original published paper.

Observation of high-energy neutrinos from the Galactic plane

The IceCube Collaboration

(a complete list of authors can be found at the end of the proceedings)

E-mail: ssclafani@icecube.wisc.edu, mhuenefeld@icecube.wisc.edu

IceCube has discovered a flux of astrophysical neutrinos and presented evidence for the first neutrino sources, a flaring blazar known as TXS 0506+056 and the active galaxy NGC 1068. However, the sources responsible for the majority of the astrophysical neutrino flux remain elusive. In addition to hypothetical sources within our Galaxy, high energy neutrinos are produced when cosmic rays interact at their acceleration sites and during propagation through the interstellar medium. The Galactic plane has therefore long been hypothesized as a neutrino source. In this contribution, new results are presented for searches of neutrino sources utilizing a dataset that builds upon recent advances in deep-learning-based reconstruction methods for neutrino-induced cascades. This work presents the first observation of high-energy neutrinos from the Milky Way Galaxy, rejecting the background-only hypothesis at 4.5σ . The neutrino signal is consistent with diffuse emission from the Galactic plane, potentially in combination with emission by a population of sources.

Corresponding authors: Steve Sclafani^{1*}, Mirco Hünnefeld²

¹ *University of Maryland*

² *TU Dortmund University*

* Presenter

The 38th International Cosmic Ray Conference (ICRC2023)
26 July – 3 August, 2023
Nagoya, Japan



1. Neutrino Production in the Milky Way

The Milky Way Galaxy has been observed over many wavelengths of light, from radio waves to gamma rays. At energies above 1 GeV, the sky as observed by *Fermi*-LAT [1] is dominated by emission from the Galactic plane of the Milky Way. Cosmic rays can interact at their acceleration site creating high-energy neutrinos and gamma rays, but can also escape the acceleration environment. The cosmic rays will generally diffuse through the Galaxy, and may interact with the dust and gas of the plane, producing emission at the site of these interactions. The observed emission reflects the density and energy of cosmic rays, as well as the column density of matter. This diffuse emission has been observed in gamma rays [1–3], and the counterpart has been predicted in high-energy neutrinos [4, 5]. This work presents the first evidence of high-energy neutrinos from the Milky Way Galaxy [6].

The IceCube Neutrino Observatory, a cubic-kilometer detector located in the geographic South Pole, is instrumented with 5160 Digital Optical Modules (DOMs), each with a PMT and digitizing hardware. When a neutrino interacts with the ice, charged secondary particles produce Cherenkov light in the detector that can be used to reconstruct the direction and energy of the primary neutrino. These interactions occur in two main topologies. “Track” events are mostly produced from “charged-current” (CC) ν_μ interactions that produce an outgoing muon, which traverses the detector and deposits light along the particle track, whereas “cascade” events are produced from “neutral-current” (NC) interactions of all flavors, as well as CC- ν_e or CC- ν_τ interactions. These produce a shower of particles that appear as a nearly spherically expanding light front. For this reason, typical cascade events have inferior angular resolution ($>10^\circ$ at 10 TeV) when compared to track events ($<1^\circ$). After IceCube discovered a flux of astrophysical neutrinos [7], it used track events to present evidence for two sources [8, 9]. The sources responsible for the majority of the astrophysical flux, however, remain unknown. The diffuse flux from the Galactic plane can account for up to $\sim 10\%$ of this flux at TeV energies [10].

Previous searches for emission from the Galactic plane did not find any significant emission [10–13]. The level of Galactic emission is expected to be low when compared to the measured all-sky astrophysical flux, and due to the direction of the Galactic center, diffuse emission is concentrated in the southern sky. For IceCube, due to the location of the detector at the South Pole, selections in the southern celestial sky are composed of events downgoing in the detector. Searches in this region are particularly difficult due to the large background of atmospheric muons. Through-going track-based analyses see a reduction of sensitivity due to this irreducible background [14]. This is especially true for galactic sources, which are assumed to follow a softer spectrum. This work, however, makes use of cascade events, which have a much reduced background in the southern sky, and lead to an improvement of sensitivity. Further, machine learning techniques applied to IceCube cascade events improve the sensitivity by a factor of 3–4 over previous searches [6]. Consequently, this work improves sensitivity to diffuse Galactic plane emission models, leading to the first evidence of high-energy neutrino emission from the Milky Way at a significance of 4.5σ .

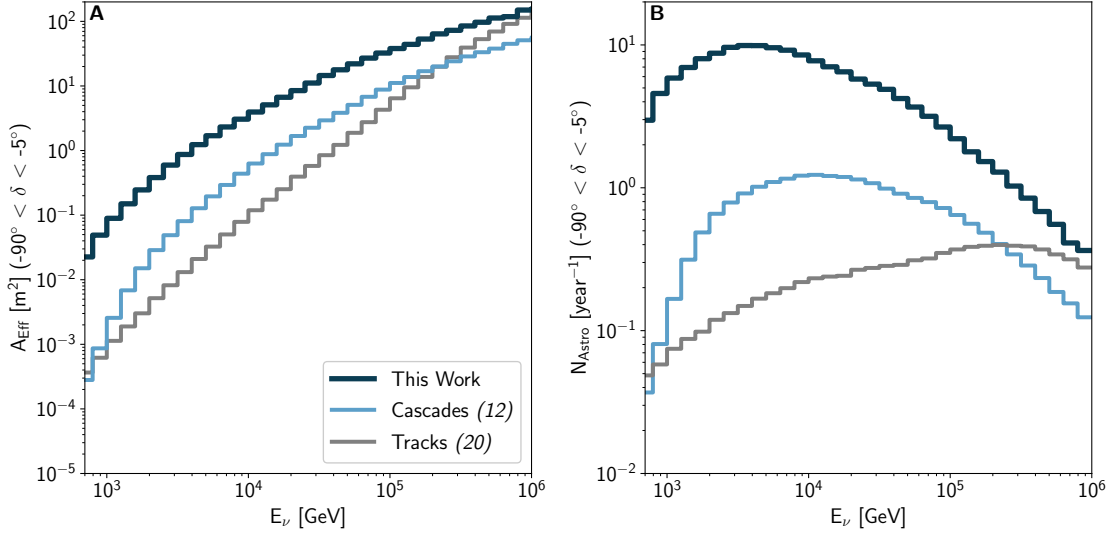


Figure 1: (A) The all-flavor southern sky effective area (A_{Eff}) of the IceCube dataset, averaged over solid angle in the declination (δ) range between -90° and -5° as a function of E_ν , the true neutrino energy. Results are shown for the deep learning event selection used in this work, (dark blue), a previous cascade event selection [12] (light blue), and, as an example, a previous though-going track event selection [14] (grey) applied to the IceCube data. (B) The number of expected signal events (N_{Astro}) in the southern sky per energy bin per year for each event selection, assuming an isotropic astrophysical flux [17]. Calculations are based on equal contributions of each neutrino flavor at Earth due to neutrino oscillations, (figure from [6])

2. Application of Deep Learning to Cascade Events

In the southern sky, the primary background for IceCube consists of atmospheric muons, which trigger the detector at a rate a billion times higher than astrophysical neutrinos. This background appears in the detector as downgoing track events which pass through the detector. These events cannot be distinguished from neutrino-induced muons entering the detector. Thus, the event selection in this work is optimized to search for events that start within the detector and have cascade-like topologies. The selection of cascade events instead of track events reduces the atmospheric muon background, and also suppresses the atmospheric neutrino background, which primarily consists of muon flavored neutrinos. Previous cascade searches [12] used an event selection based on veto layers that improved the effective area over tracks in the 1-100 TeV range [15]. This work, however, relies heavily on a Deep-Neural-Network (DNN) based selection [16] that improves the selection efficiency [6] at low energies. Further, this work includes events that are partially contained within the detector, which improves the efficiency mostly at higher energies. Due to the reduced backgrounds, the lower energy threshold is pushed lower, from a tens of TeV down to around 1 TeV. The effective area at 10 TeV is increased by a factor of ~ 5 when compared to previous cascade selections, as shown in Figure 1A. This increase in effective area corresponds to an increase of astrophysical events by up to a factor of 20, assuming the measurement in [17], as shown in Figure 1B. Relative improvements are largest at energies below a few tens of TeV.

The event selection also relies on a novel reconstruction that combines the advantages of DNNs

with traditional maximum likelihood methods [18]. The new reconstruction technique results in a similar, sample-averaged angular resolution at high energies as obtained by the previous cascade sample, despite the inclusion of more challenging events. At low energies, the sample-averaged resolution is improved by up to a factor of two. These improvements are achieved due to better exploitation of available information and symmetries in the novel reconstruction method [18].

3. Searches for Galactic neutrino emission

Multiple source hypotheses were tested. The focus of this work is the testing of three models of diffuse Galactic plane emission. The first model, referred to here as π^0 , is based on the extrapolation from the *Fermi*-LAT fit to the first 21 months of data [1]. The spatial template from *Fermi*-LAT is assumed unchanged at TeV energies, and the energy spectrum is assumed to be an unbroken power-law with fixed spectral index $\gamma=2.7$. The other two models, referred to as KRA_γ , model the Galactic cosmic ray diffusion coefficient as radially dependent [19]. This results in a harder spectrum towards the galactic center which then results in an enhanced flux after extrapolation to IceCube's energies. Here we test the extrapolated flux, but use a global energy dependant spectrum, averaged over all directions. Two cutoffs are tested. KRA_γ^5 and KRA_γ^{50} correspond to cutoffs in Galactic cosmic rays at 5 PeV and 50 PeV respectively. These energies are propagated down to lower energies in neutrinos. The sky-integrated flux of these models are shown in Figure 2.

For each template, the number of signal events is fitted while the spectrum is held fixed. A likelihood-ratio test is performed with the log-likelihood ratio as the test statistic (TS) [11]. Background TS distributions are calculated from scrambled data, and the true TS for each template is compared with this background distribution to calculate the p-value. Due to IceCube's location on the Earth, scrambling the Right Ascension (RA) direction produces background-like pseudo-experiments, but preserves any detector effects. Using this data driven technique to derive p-values, any unmodeled effect will result in a reduction of sensitivity, but not risk a false signal.

In addition to the diffuse Galactic plane analyses, searches were performed for neutrino emission from Galactic source classes corresponding to supernova remnants (SNR), pulsar wind nebulae (PWN) and unidentified TeV gamma-ray sources (UNID). Stacking sources can result in an improved sensitivity over searching for each source individually. Three classes of 12 potential Galactic sources are selected based on their TeV gamma-ray flux, and each is source is weighted to equally contribute. The complete source list is available in Ref. [6].

4. Neutrinos from the Milky Way

The results for the diffuse Galactic plane and source stacking are shown in Table 1 and Table 2 respectively, which was first reported in [6]. Each of the diffuse emission hypotheses is significant with pre-trial p-values corresponding to 4.71σ , 4.37σ and 3.96σ , respectively. These fluxes correspond to best-fitting values of 748, 276, and 211 signal events (n_s) in the IceCube dataset for the π^0 , KRA_γ^5 and KRA_γ^{50} models, respectively. After accounting for the three tested hypotheses, the resulting post-trials p-value is calculated, and corresponds to a significance of 4.5σ .

Also included in Table 1 are best-fit flux normalizations for each template. The π^0 flux is reported at 100 TeV. Since the KRA_γ models do not follow a power-law, the flux is reported as

Diffuse Galactic plane analyses	Flux Sensitivity Φ	Best-fitting n_s	p-value	Best-fitting flux Φ
π^0	5.98	748	1.3×10^{-6} (4.71σ)	$21.8^{+5.3}_{-4.9}$
KRA_γ^5	$0.16 \times \text{MF}$	276	6.1×10^{-6} (4.37σ)	$0.55^{+0.18}_{-0.15} \times \text{MF}$
KRA_γ^{50}	$0.11 \times \text{MF}$	211	3.7×10^{-5} (3.96σ)	$0.37^{+0.13}_{-0.11} \times \text{MF}$

Table 1: The flux sensitivity and best-fitting flux normalization (Φ) are given in units of model flux (MF) for KRA_γ templates and as $E^2 \frac{dN}{dE}$ at 100 TeV in units of 10^{-12} TeV cm $^{-2}$ s $^{-1}$ for the π^0 analyses ($\frac{dN}{dE}$ is the differential number of neutrinos per flavor, N, and neutrino energy, E). P-values and significance are calculated with respect to the background-only hypothesis. Pre-trial p-values for each individual result are shown for the three diffuse Galactic plane analyses.

Catalog	Sensitivity Φ	n_s	γ	p-value	Significance (σ)	Flux Φ	UL Φ
SNR	2.24	218.6	2.75	5.9×10^{-4}	3.24	6.22	<9.01
PWN	2.25	279.6	3.00	5.9×10^{-4}	3.24	3.80	<9.50
UNID	1.89	238.4	2.85	3.4×10^{-4}	3.40	5.03	<7.76

Table 2: Pre-trial significance, sensitivity, best-fitting spectrum (γ), total number of signal events (n_s), flux, and 90% Upper Limits (UL) for the Galactic stacking catalog analyses. Upper limits are with respect to a source emitting following an E^{-2} spectrum. The per-flavor neutrino flux sensitivity, best-fit, and upper limits are given as $E^2 \frac{dN}{dE}$ at 100 TeV in units of 10^{-12} TeV cm $^{-2}$ s $^{-1}$ for the entire catalog of sources.

multiples of the model prediction. Those normalizations are shown compared to the model for each template in Figure 2. The KRA_γ best-fitting normalization is less than the models, whereas the π^0 best-fit is larger by a factor of ~ 5 than the π^0 model. This could be an indication that the underlying diffuse emission spectrum is more complex than assumed in any of the tested models, possibly containing a contribution from unresolved Galactic sources. These results are based on the all-sky template and model-to-model flux comparisons depend on the considered sky region. When considering regions of the sky tested by gamma-ray experiments like Tibet-AS γ the best-fit π^0 model fits well with the measured gamma-ray flux. The IceCube result, however, is a measurement over the entire sky and it does not attempt to mask out any galactic sources, as none have been identified.

In addition to the Galactic diffuse templates, the three Galactic stacking analyses also resulted in evidence above 3σ with pre-trial significance of 3.24σ , 3.24σ , and 3.40σ for the SNR, PWN, and UNID classes respectively. The full results are shown in Table 2. Due to the large spatial overlap in source hypotheses, these significances are expected in the scenario of diffuse emission at the best-fit values reported in Table 1. This analysis cannot distinguish the contribution of individual sources or classes of sources from diffuse emission.

Finally, an all-sky scan was performed, searching at each location on the sky for an excess of point-like neutrino emission. The visualization of this all-sky search is shown in equatorial coordinates in Figure 3. Excesses are visible along the Galactic plane and near well known gamma-ray emitters, such as the Crab Nebula, 3C 454.3, and the Cygnus X region, however, no single point is significant once trials are accounted for.

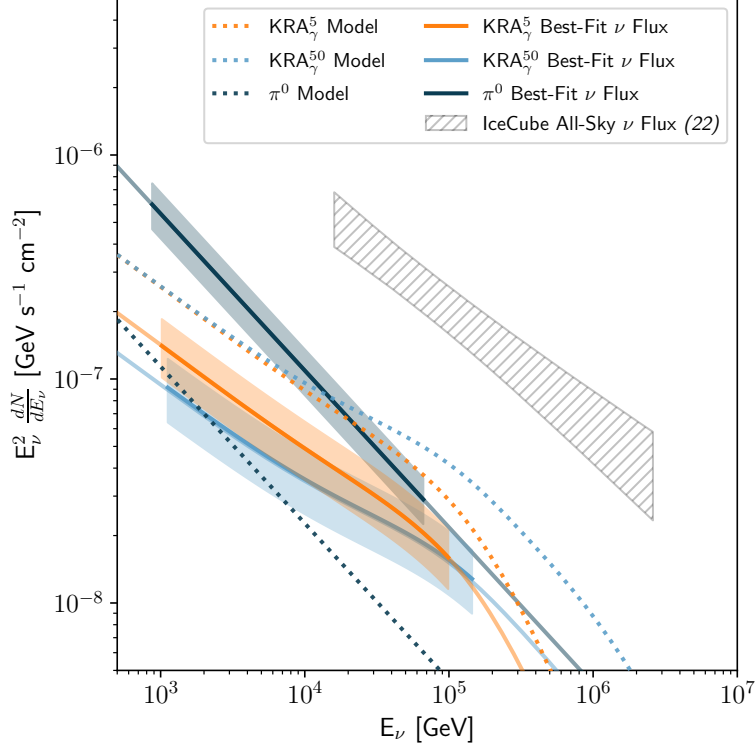


Figure 2: Energy-scaled, sky-integrated, per-flavor neutrino flux as a function of neutrino energy (E_ν) for each of the Galactic plane models. Dotted lines are the predicted values for the π^0 (dark blue), KRA_γ^5 (orange) and KRA_γ^{50} (light blue) models while solid lines are our best-fitting flux normalizations from the IceCube data. Shaded regions indicate the 1σ uncertainties, extending over the energy range that contributes to 90% of the significance. These results are based on the all-sky (4π sr) template and are presented as an all-sky flux. For comparison, the grey hatching shows the flux of the IceCube all-sky neutrino flux [17], scaled to an all-sky flux by multiplying by 4π , with its 1σ uncertainty. Figure from [6]

5. Conclusion

This work presents the first evidence of high-energy neutrino emission from the Milky Way Galaxy. The result is consistent with a diffuse neutrino emission hypothesis or a collection of unresolved sources.

Round-trip tests were performed to investigate the correlation between the source stacking analyses and the diffuse Galactic plane analyses. Injecting the best-fitted flux from the π^0 template results in a significance for the other templates that is compatible with the observed results. Injecting any one of the stacking source hypotheses individually, does not recover the best-fitted flux for the diffuse emission models. Further, it is possible that some of these sources still contribute to the observed flux.

More information is needed to characterize the Galactic component of the astrophysical neutrino flux. A larger range of Galactic templates, including more recent models [20], have been tested with a dataset of northern sky track events in IceCube [21]. A search for the same diffuse templates was also performed with IceCube starting track events [22, 23]. Both results are compatible with

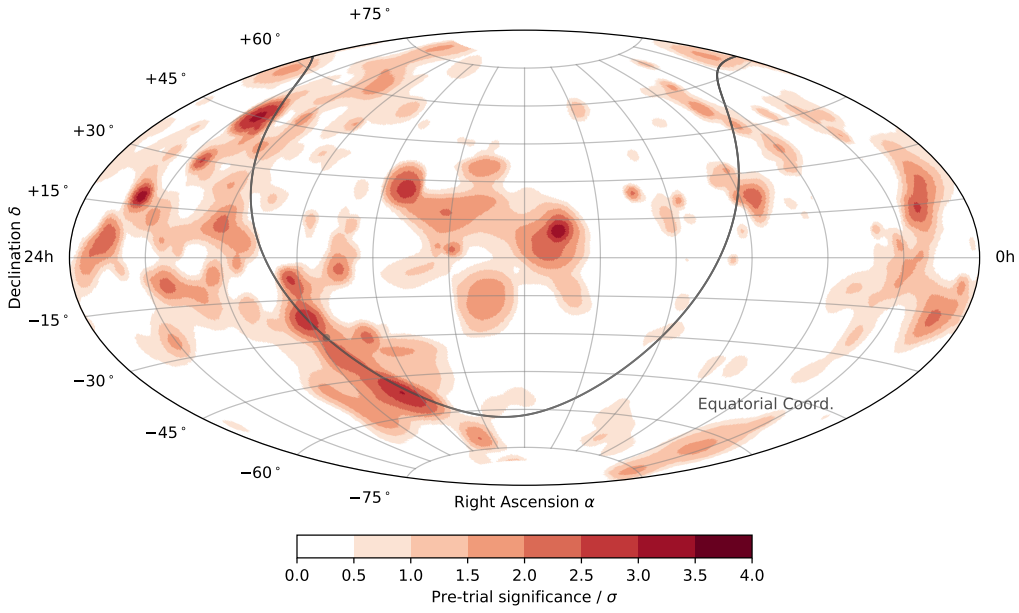


Figure 3: The best-fitting pre-trial significance for the all-sky search is shown as a function of direction in an Aitoff projection of the celestial sphere, in equatorial coordinates (J2000 equinox). The Galactic plane is indicated by a grey curve, and the Galactic Center as a dot. Although some locations appear to have significant emission, the trial factor for the number of points searched means these points are all individually statistically consistent with background fluctuations. The clustering of larger significances along the galactic plane reflects the significant excess that is observed in the template searches for the Galactic plane. Figure from [6].

the results presented in this work. Further work will require the identification of sources and their spectra. This could be done by combining the signal purity of cascade events with the angular resolution of track events [24].

References

- [1] *Fermi-LAT* Collaboration, M. Ackermann *et al.* *Astrophys. J.* **750** no. 1, (Apr, 2012) 3.
- [2] Z. Cao *et al.* [arXiv:2305.05372](https://arxiv.org/abs/2305.05372).
- [3] *Tibet AS_γ* Collaboration, M. Amenomori *et al.* *Phys. Rev. Lett.* **126** (Apr, 2021) 141101.
- [4] F. W. Stecker *Astrophys. J.* **228** (Mar., 1979) 919–927.
- [5] V. Berezhinsky *et al.* *Astropart. Phys.* **1** no. 3, (1993) 281–287.
- [6] *IceCube* Collaboration, R. Abbasi *et al.* *Science* **380** no. 6652, (2023) .
- [7] *IceCube* Collaboration *Science* **342** no. 6161, (2013) 1242856.
- [8] *IceCube* Collaboration, M. Aartsen *et al.* *Science* **361** no. 6398, (2018) 147–151.
- [9] *IceCube* Collaboration, R. Abbasi *et al.* *Science* **378** no. 6619, (2022) 538–543.

- [10] A. Albert *et al.* *The Astrophysical Journal* **868** no. 2, (Nov., 2018) L20.
- [11] **IceCube** Collaboration, M. G. Aartsen *et al.* *Astrophys. J.* **849** no. 1, (Oct, 2017) 67.
- [12] **IceCube** Collaboration, M. G. Aartsen *et al.* *Astrophys. J.* **886** no. 1, (Nov, 2019) 12.
- [13] **ANTARES** Collaboration, A. Albert *et al.* *Physics Letters B* **841** (June, 2023) 137951.
- [14] **IceCube** Collaboration, M. Aartsen *et al.* *Physical Review Letters* **124** no. 5, (Feb., 2020) .
- [15] **IceCube** Collaboration, M. G. Aartsen *et al.* *Phys. Rev. D* **91** (Jan., 2015) 022001.
- [16] **IceCube** Collaboration, R. Abbasi *et al.* *J. Instrum.* **16** no. 07, (July, 2021) P07041.
- [17] **IceCube** Collaboration, M. G. Aartsen *et al.* *Phys. Rev. Lett.* **125** no. 12, (Sep, 2020) 121104.
- [18] **IceCube** Collaboration, M. Huennefeld, R. Abbasi, *et al.* *PoS ICRC2021* (2021) 1065.
- [19] D. Gaggero *et al.* *Astrophys. J.* **815** no. 2, (Dec, 2015) L25.
- [20] G. Schwefer, P. Mertsch, and C. Wiebusch *The Astrophysical Journal* **949** no. 1, (May, 2023) 16.
- [21] **IceCube** Collaboration *PoS ICRC2023* (these proceedings) 1046.
- [22] **IceCube** Collaboration *PoS ICRC2023* (these proceedings) 1008.
- [23] **IceCube** Collaboration, M. G. Aartsen *et al.* *To be submitted to Physical Review D* .
- [24] **IceCube** Collaboration *PoS ICRC2023* (these proceedings) 1010.

Full Author List: IceCube Collaboration

R. Abbasi¹⁷, M. Ackermann⁶³, J. Adams¹⁸, S. K. Agarwalla^{40, 64}, J. A. Aguilar¹², M. Ahlers²², J.M. Alameddine²³, N. M. Amin⁴⁴, K. Andeen⁴², G. Anton²⁶, C. Argüelles¹⁴, Y. Ashida⁵³, S. Athanasiadou⁶³, S. N. Axani⁴⁴, X. Bai⁵⁰, A. Balagopal V.⁴⁰, M. Baricevic⁴⁰, S. W. Barwick³⁰, V. Basu⁴⁰, R. Bay⁸, J. J. Beatty^{20, 21}, J. Becker Tjus^{11, 65}, J. Beise⁶¹, C. Bellenghi²⁷, C. Benning¹, S. BenZvi⁵², D. Berley¹⁹, E. Bernardini⁴⁸, D. Z. Besson³⁶, E. Blaufuss¹⁹, S. Blot⁶³, F. Bontempo³¹, J. Y. Book¹⁴, C. Boscolo Meneguolo⁴⁸, S. Böser⁴¹, O. Botner⁶¹, J. Böttcher⁷, E. Bourbeau²², J. Braun⁴⁰, B. Brinson⁶, J. Brostean-Kaiser⁶³, R. T. Burley², R. S. Busse⁴³, D. Butterfield⁴⁰, M. A. Campana⁴⁹, K. Carloni¹⁴, E. G. Carnie-Bronca², S. Chattopadhyay^{40, 64}, N. Chau¹², C. Chen⁶, Z. Chen⁵⁵, D. Chirkin⁴⁰, S. Choi⁵⁶, B. A. Clark¹⁹, L. Classen⁴³, A. Coleman⁶¹, G. H. Collin¹⁵, A. Connolly^{20, 21}, J. M. Conrad¹⁵, P. Coppin¹³, P. Correa¹³, D. F. Cowen^{59, 60}, P. Dave⁶, C. De Clercq¹³, J. J. DeLaunay⁵⁸, D. Delgado¹⁴, S. Deng¹, K. Deoskar⁵⁴, A. Desai⁴⁰, P. Desati⁴⁰, K. D. de Vries¹³, G. de Wasseige³⁷, T. DeYoung²⁴, A. Diaz¹⁵, J. C. Díaz-Vélez⁴⁰, M. Dittmer⁴³, A. Domi²⁶, H. Dujmovic⁴⁰, M. A. DuVernois⁴⁰, T. Ehrhardt⁴¹, P. Eller²⁷, E. Ellinger⁶², S. El Mentawi¹, D. Elsässer²³, R. Engel^{31, 32}, H. Erpenbeck⁴⁰, J. Evans¹⁹, P. A. Evenson⁴⁴, K. L. Fan¹⁹, K. Fang⁴⁰, K. Farrag¹⁶, A. R. Farrag¹⁶, A. Fedynitch⁵⁷, N. Feigl¹⁰, S. Fiedlschuster²⁶, C. Finley⁵⁴, L. Fischer⁶⁷, D. Fox⁵⁹, A. Frankowiak¹¹, A. Fritz⁴¹, P. Fürst¹, J. Gallagher³⁹, E. Ganster¹, A. Garcia¹⁴, L. Gerhardt⁹, A. Ghadimi⁵⁸, C. Glaser⁶¹, T. Glauch²⁷, T. Glüsenskamp^{26, 61}, N. Goehke³², J. G. Gonzalez⁴⁴, S. Goswami⁵⁸, D. Grant²⁴, S. J. Gray¹⁹, O. Gries¹, S. Griffin⁴⁰, S. Griswold⁵², K. M. Groth²², C. Günther¹, P. Gutjahr²³, C. Haack²⁶, A. Hallgren⁶¹, R. Halliday²⁴, L. Halve¹, F. Halzen⁴⁰, H. Hamdaoui⁵⁵, M. Ha Minh²⁷, K. Hanson⁴⁰, J. Hardin¹⁵, A. A. Harnisch²⁴, P. Hatch³³, A. Haungs³¹, K. Helbing⁶², J. Hellrung¹¹, F. Henningsen²⁷, L. Heuermann¹, N. Heyer⁶¹, S. Hickford⁶², A. Hidvegi⁵⁴, C. Hill¹⁶, G. C. Hill², K. D. Hoffman¹⁹, S. Hori⁴⁰, K. Hoshina^{40, 66}, W. Hou³¹, T. Huber³¹, K. Hultqvist⁵⁴, M. Hünnefeld²³, R. Hussain⁴⁰, K. Hymon²³, S. In⁵⁶, A. Ishihara¹⁶, M. Jacquart¹⁶, O. Janik¹, M. Jansson⁵⁴, G. S. Japaridze⁵, M. Jeong⁵⁶, M. Jin¹⁴, B. J. P. Jones⁴, D. Kang³¹, W. Kang⁵⁶, X. Kang⁴⁹, A. Kappes⁴³, D. Kappesser⁴¹, L. Kardum²³, T. Karg⁶³, M. Karle²⁷, A. Karle⁴⁰, U. Katz²⁶, M. Kauer⁴⁰, J. L. Kelley⁴⁰, A. Khatee Zathul⁴⁰, A. Kheirandish^{34, 35}, J. Kiryluk⁵⁵, S. R. Klein^{8, 9}, A. Kochocki²⁴, R. Koirala⁴⁴, H. Kolanoski¹⁰, T. Kontrimas²⁷, L. Köpke⁴¹, C. Kopper²⁶, D. J. Koskinen²², P. Koundal³¹, M. Kovacevich⁴⁹, M. Kowalski^{10, 63}, T. Kozynets²², J. Krishnamoorthi^{40, 64}, K. Kruijswijk³⁷, E. Krupczak²⁴, A. Kumar⁶³, E. Kun¹¹, N. Kurahashi⁴⁹, N. Lad⁶³, C. Lagunas Gualda⁶³, M. Lamoureux³⁷, M. J. Larson¹⁹, S. Latseva¹, F. Lauber⁶², J. P. Lazar^{14, 40}, J. W. Lee⁵⁶, K. Leonard DeHolton⁶⁰, A. Leszczyńska⁴⁴, M. Lincetto¹¹, Q. R. Liu⁴⁰, M. Liubarska²⁵, E. Lohfink⁴¹, C. Love⁴⁹, C. J. Lozano Mariscal⁴³, L. Lu⁴⁰, F. Lucarelli²⁸, W. Luszczyk^{20, 21}, Y. Lyu^{8, 9}, J. Madsen⁴⁰, K. B. M. Mahn²⁴, Y. Makino⁴⁰, E. Manao²⁷, S. Mancina^{40, 48}, W. Marie Sainte⁴⁰, I. C. Mariş¹², S. Marka⁴⁶, Z. Marka⁴⁶, M. Marsee⁵⁸, I. Martinez-Soler¹⁴, R. Maruyama⁴⁵, F. Mayhew²⁴, T. McElroy²⁵, F. McNally³⁸, J. V. Mead²², K. Meagher⁴⁰, S. Mechbal⁶³, A. Medina²¹, M. Meier¹⁶, Y. Merckx¹³, L. Merten¹¹, J. Micallef²⁴, J. Mitchell⁷, T. Montaruli²⁸, R. W. Moore²⁵, Y. Morii¹⁶, R. Morse⁴⁰, M. Moulai⁴⁰, T. Mukherjee³¹, R. Naab⁶³, R. Nagai¹⁶, M. Nakos⁴⁰, U. Naumann⁶², J. Necker⁶³, A. Negi⁴, M. Neumann⁴³, H. Niederhausen²⁴, M. U. Nisa²⁴, A. Noell¹, A. Novikov⁴⁴, S. C. Nowicki²⁴, A. Obertacke Pollmann¹⁶, V. O'Dell⁴⁰, M. Oehler³¹, B. Oeyen²⁹, A. Olivas¹⁹, R. Ørsøe²⁷, J. Osborn⁴⁰, E. O'Sullivan⁶¹, H. Pandya⁴⁴, N. Park³³, G. K. Parker⁴, E. N. Paudel⁴⁴, L. Paul^{42, 50}, C. Pérez de los Heros⁶¹, J. Peterson⁴⁰, S. Philippen¹, A. Pizzuto⁴⁰, M. Plum⁵⁰, A. Pontén⁶¹, Y. Popovych⁴¹, M. Prado Rodriguez⁴⁰, B. Pries²⁴, R. Procter-Murphy¹⁹, G. T. Przybylski⁹, C. Raab³⁷, J. Rack-Helleis⁴¹, K. Rawlins³, Z. Rechav⁴⁰, A. Rehman⁴⁴, P. Reichherzer¹¹, G. Renzi¹², E. Resconi²⁷, S. Reusch⁶³, W. Rhode²³, B. Riedel⁴⁰, A. Rifaie¹, E. J. Roberts², S. Robertson^{8, 9}, S. Rodan⁵⁶, G. Roellinghoff⁵⁶, M. Rongen²⁶, C. Rott^{53, 56}, T. Ruhe²³, L. Ruohan²⁷, D. Ryckbosch²⁹, I. Safa^{14, 40}, J. Saffer³², D. Salazar-Gallegos²⁴, P. Sampathkumar³¹, S. E. Sanchez Herrera²⁴, A. Sandrock⁶², M. Santander⁵⁸, S. Sarkar²⁵, S. Sarkar⁴⁷, J. Savelberg¹, P. Savina⁴⁰, M. Schaufel¹, H. Schieler³¹, S. Schindler²⁶, L. Schlickmann¹, B. Schlüter⁴³, F. Schlüter¹², N. Schmeisser⁶², T. Schmidt¹⁹, J. Schneider²⁶, F. G. Schröder^{31, 44}, L. Schumacher²⁶, G. Schwefer¹, S. Sclafani¹⁹, D. Seckel⁴⁴, M. Seikh³⁶, S. Seunarine⁵¹, R. Shah⁴⁹, A. Sharma⁶¹, S. Shefali³², N. Shimizu¹⁶, M. Silva⁴⁰, B. Skrzypek¹⁴, B. Smithers⁴, R. Snihur⁴⁰, J. Soedingrekso²³, A. Sogaard²², D. Soldin³², P. Soldin¹, G. Sommani¹¹, C. Spannfellner²⁷, G. M. Spiczak⁵¹, C. Spiering⁶³, M. Stamatikos²¹, T. Stanev⁴⁴, T. Stetzelberger⁹, T. Stürwald⁶², T. Stuttard²², G. W. Sullivan¹⁹, I. Taboada⁶, S. Ter-Antonyan⁷, M. Thiesmeyer¹, W. G. Thompson¹⁴, J. Thwaites⁴⁰, S. Tilav⁴⁴, K. Tollefson²⁴, C. Tönnis⁵⁶, S. Toscano¹², D. Tosi⁴⁰, A. Trettin⁶³, C. F. Tung⁶, R. Turcotte³¹, J. P. Twagirayezu²⁴, B. Ty⁴⁰, M. A. Unland Elorrieta⁴³, A. K. Upadhyay^{40, 64}, K. Uphaw⁷, N. Valtonen-Mattila⁶¹, J. Vandenbroucke⁴⁰, N. van Eijndhoven¹³, D. Vannerom¹⁵, J. van Santen⁶³, J. Vara⁴³, J. Veitch-Michaelis⁴⁰, M. Venugopal³¹, M. Vereecken³⁷, S. Verpoest⁴⁴, D. Veske⁴⁶, A. Vijai¹⁹, C. Walck⁵⁴, C. Weaver²⁴, P. Weigel¹⁵, A. Weindl³¹, J. Weldert⁶⁰, C. Wendt⁴⁰, J. Werthebach²³, M. Weyrauch³¹, N. Whitehorn²⁴, C. H. Wiebusch¹, N. Willey²⁴, D. R. Williams⁵⁸, L. Witthaus²³, A. Wolf¹, M. Wolf²⁷, G. Wrede²⁶, X. W. Xu⁷, J. P. Yanez²⁵, E. Yildizci⁴⁰, S. Yoshida¹⁶, R. Young³⁶, F. Yu¹⁴, S. Yu²⁴, T. Yuan⁴⁰, Z. Zhang⁵⁵, P. Zhelnin¹⁴, M. Zimmerman⁴⁰

¹ III. Physikalisches Institut, RWTH Aachen University, D-52056 Aachen, Germany

² Department of Physics, University of Adelaide, Adelaide, 5005, Australia

³ Dept. of Physics and Astronomy, University of Alaska Anchorage, 3211 Providence Dr., Anchorage, AK 99508, USA

⁴ Dept. of Physics, University of Texas at Arlington, 502 Yates St., Science Hall Rm 108, Box 19059, Arlington, TX 76019, USA

⁵ CTSPS, Clark-Atlanta University, Atlanta, GA 30314, USA

⁶ School of Physics and Center for Relativistic Astrophysics, Georgia Institute of Technology, Atlanta, GA 30332, USA

⁷ Dept. of Physics, Southern University, Baton Rouge, LA 70813, USA

⁸ Dept. of Physics, University of California, Berkeley, CA 94720, USA

⁹ Lawrence Berkeley National Laboratory, Berkeley, CA 94720, USA

¹⁰ Institut für Physik, Humboldt-Universität zu Berlin, D-12489 Berlin, Germany

¹¹ Fakultät für Physik & Astronomie, Ruhr-Universität Bochum, D-44780 Bochum, Germany

¹² Université Libre de Bruxelles, Science Faculty CP230, B-1050 Brussels, Belgium

- ¹³ Vrije Universiteit Brussel (VUB), Dienst ELEM, B-1050 Brussels, Belgium
¹⁴ Department of Physics and Laboratory for Particle Physics and Cosmology, Harvard University, Cambridge, MA 02138, USA
¹⁵ Dept. of Physics, Massachusetts Institute of Technology, Cambridge, MA 02139, USA
¹⁶ Dept. of Physics and The International Center for Hadron Astrophysics, Chiba University, Chiba 263-8522, Japan
¹⁷ Department of Physics, Loyola University Chicago, Chicago, IL 60660, USA
¹⁸ Dept. of Physics and Astronomy, University of Canterbury, Private Bag 4800, Christchurch, New Zealand
¹⁹ Dept. of Physics, University of Maryland, College Park, MD 20742, USA
²⁰ Dept. of Astronomy, Ohio State University, Columbus, OH 43210, USA
²¹ Dept. of Physics and Center for Cosmology and Astro-Particle Physics, Ohio State University, Columbus, OH 43210, USA
²² Niels Bohr Institute, University of Copenhagen, DK-2100 Copenhagen, Denmark
²³ Dept. of Physics, TU Dortmund University, D-44221 Dortmund, Germany
²⁴ Dept. of Physics and Astronomy, Michigan State University, East Lansing, MI 48824, USA
²⁵ Dept. of Physics, University of Alberta, Edmonton, Alberta, Canada T6G 2E1
²⁶ Erlangen Centre for Astroparticle Physics, Friedrich-Alexander-Universität Erlangen-Nürnberg, D-91058 Erlangen, Germany
²⁷ Technical University of Munich, TUM School of Natural Sciences, Department of Physics, D-85748 Garching bei München, Germany
²⁸ Département de physique nucléaire et corpusculaire, Université de Genève, CH-1211 Genève, Switzerland
²⁹ Dept. of Physics and Astronomy, University of Gent, B-9000 Gent, Belgium
³⁰ Dept. of Physics and Astronomy, University of California, Irvine, CA 92697, USA
³¹ Karlsruhe Institute of Technology, Institute for Astroparticle Physics, D-76021 Karlsruhe, Germany
³² Karlsruhe Institute of Technology, Institute of Experimental Particle Physics, D-76021 Karlsruhe, Germany
³³ Dept. of Physics, Engineering Physics, and Astronomy, Queen's University, Kingston, ON K7L 3N6, Canada
³⁴ Department of Physics & Astronomy, University of Nevada, Las Vegas, NV, 89154, USA
³⁵ Nevada Center for Astrophysics, University of Nevada, Las Vegas, NV 89154, USA
³⁶ Dept. of Physics and Astronomy, University of Kansas, Lawrence, KS 66045, USA
³⁷ Centre for Cosmology, Particle Physics and Phenomenology - CP3, Université catholique de Louvain, Louvain-la-Neuve, Belgium
³⁸ Department of Physics, Mercer University, Macon, GA 31207-0001, USA
³⁹ Dept. of Astronomy, University of Wisconsin–Madison, Madison, WI 53706, USA
⁴⁰ Dept. of Physics and Wisconsin IceCube Particle Astrophysics Center, University of Wisconsin–Madison, Madison, WI 53706, USA
⁴¹ Institute of Physics, University of Mainz, Staudinger Weg 7, D-55099 Mainz, Germany
⁴² Department of Physics, Marquette University, Milwaukee, WI, 53201, USA
⁴³ Institut für Kernphysik, Westfälische Wilhelms-Universität Münster, D-48149 Münster, Germany
⁴⁴ Bartol Research Institute and Dept. of Physics and Astronomy, University of Delaware, Newark, DE 19716, USA
⁴⁵ Dept. of Physics, Yale University, New Haven, CT 06520, USA
⁴⁶ Columbia Astrophysics and Nevis Laboratories, Columbia University, New York, NY 10027, USA
⁴⁷ Dept. of Physics, University of Oxford, Parks Road, Oxford OX1 3PU, United Kingdom
⁴⁸ Dipartimento di Fisica e Astronomia Galileo Galilei, Università Degli Studi di Padova, 35122 Padova PD, Italy
⁴⁹ Dept. of Physics, Drexel University, 3141 Chestnut Street, Philadelphia, PA 19104, USA
⁵⁰ Physics Department, South Dakota School of Mines and Technology, Rapid City, SD 57701, USA
⁵¹ Dept. of Physics, University of Wisconsin, River Falls, WI 54022, USA
⁵² Dept. of Physics and Astronomy, University of Rochester, Rochester, NY 14627, USA
⁵³ Department of Physics and Astronomy, University of Utah, Salt Lake City, UT 84112, USA
⁵⁴ Oskar Klein Centre and Dept. of Physics, Stockholm University, SE-10691 Stockholm, Sweden
⁵⁵ Dept. of Physics and Astronomy, Stony Brook University, Stony Brook, NY 11794-3800, USA
⁵⁶ Dept. of Physics, Sungkyunkwan University, Suwon 16419, Korea
⁵⁷ Institute of Physics, Academia Sinica, Taipei, 11529, Taiwan
⁵⁸ Dept. of Physics and Astronomy, University of Alabama, Tuscaloosa, AL 35487, USA
⁵⁹ Dept. of Astronomy and Astrophysics, Pennsylvania State University, University Park, PA 16802, USA
⁶⁰ Dept. of Physics, Pennsylvania State University, University Park, PA 16802, USA
⁶¹ Dept. of Physics and Astronomy, Uppsala University, Box 516, S-75120 Uppsala, Sweden
⁶² Dept. of Physics, University of Wuppertal, D-42119 Wuppertal, Germany
⁶³ Deutsches Elektronen-Synchrotron DESY, Platanenallee 6, 15738 Zeuthen, Germany
⁶⁴ Institute of Physics, Sachivalaya Marg, Sainik School Post, Bhubaneswar 751005, India
⁶⁵ Department of Space, Earth and Environment, Chalmers University of Technology, 412 96 Gothenburg, Sweden
⁶⁶ Earthquake Research Institute, University of Tokyo, Bunkyo, Tokyo 113-0032, Japan

Acknowledgements

The authors gratefully acknowledge the support from the following agencies and institutions: USA – U.S. National Science Foundation-Office of Polar Programs, U.S. National Science Foundation-Physics Division, U.S. National Science Foundation-EPSCoR, Wisconsin Alumni Research Foundation, Center for High Throughput Computing (CHTC) at the University of Wisconsin–Madison, Open Science

Grid (OSG), Advanced Cyberinfrastructure Coordination Ecosystem: Services & Support (ACCESS), Frontera computing project at the Texas Advanced Computing Center, U.S. Department of Energy-National Energy Research Scientific Computing Center, Particle astrophysics research computing center at the University of Maryland, Institute for Cyber-Enabled Research at Michigan State University, and Astroparticle physics computational facility at Marquette University; Belgium – Funds for Scientific Research (FRS-FNRS and FWO), FWO Odysseus and Big Science programmes, and Belgian Federal Science Policy Office (Belspo); Germany – Bundesministerium für Bildung und Forschung (BMBF), Deutsche Forschungsgemeinschaft (DFG), Helmholtz Alliance for Astroparticle Physics (HAP), Initiative and Networking Fund of the Helmholtz Association, Deutsches Elektronen Synchrotron (DESY), and High Performance Computing cluster of the RWTH Aachen; Sweden – Swedish Research Council, Swedish Polar Research Secretariat, Swedish National Infrastructure for Computing (SNIC), and Knut and Alice Wallenberg Foundation; European Union – EGI Advanced Computing for research; Australia – Australian Research Council; Canada – Natural Sciences and Engineering Research Council of Canada, Calcul Québec, Compute Ontario, Canada Foundation for Innovation, WestGrid, and Compute Canada; Denmark – Villum Fonden, Carlsberg Foundation, and European Commission; New Zealand – Marsden Fund; Japan – Japan Society for Promotion of Science (JSPS) and Institute for Global Prominent Research (IGPR) of Chiba University; Korea – National Research Foundation of Korea (NRF); Switzerland – Swiss National Science Foundation (SNSF); United Kingdom – Department of Physics, University of Oxford.